Supermassive Stars: Fact or Fiction?

Hans-Thomas Janka

Max-Planck-Institut für Astrophysik, Karl-Schwarzschild-Str. 1, D-85741 Garching, Germany

Abstract. Supermassive black holes are now realized to exist in the centers of most galaxies. The recent discoveries of luminous quasars at redshifts higher than 6 require that these black holes were assembled already when the Universe was less than a billion years old. They might originate from the collapse of supermassive stars, a scenario which could ensure a sufficiently rapid formation. Supermassive stars are dominated by photon pressure and radiate at their Eddington limit, which drives their quasi-static evolution to a final relativistic instability. Above some critical value of the metallicity, their collapse can lead to a gigantic explosion, powered by the energy release due to hydrogen burning, but below this critical metallicity their collapse inevitably ends in the formation of a black hole, accompanied by the emission of huge amounts of energy in the form of neutrinos. Although collapsing supermassive stars are the most powerful known burst sources of neutrinos, the associated conditions do not appear favorable for producing highly relativistic outflows that can explain cosmic gamma-ray bursts.

1 Introduction

The existence of supermassive black holes (SMBHs) in most galaxies is now becoming a generally accepted fact [38]. Increasingly better resolved observations reveal large Doppler shifts of spectral lines from hot gas swirling around the galactic centers with huge velocities, indicating extraordinarily high mass concentrations in remarkably small volumes (Fig. 1). The rapid orbital motions of the stars in the cluster surrounding Sgr A* in the Milky Way require the stabilizing gravitational attraction of a dark object with a mass of about $3\times10^6\,M_\odot$ [13]. This, though, is near the lower end of the empirical mass distribution of supermassive galactic black holes. The black hole masses, the largest of which exceed $10^9\,M_\odot$, correlate with the luminosity of the elliptical-galaxy-like bulge part of the host galaxy and with the average line-of-sight random velocity ("velocity dispersion") of the stars in the host galaxy. This indictes a correlation between black hole mass and galaxy mass and is interpreted as a hint to a direct connection between galaxy formation and black hole fueling [28,34].

SMBHs with masses of a million to a few billion solar masses are believed to be the engines that power active galactic nuclei ranging from faint, compact radio sources to quasars that are brighter than the whole galaxy in which they live. The detection of quasars with redshifts larger than 6 requires that these objects were formed only several hundred million years after the Big Bang. The growth of black holes by accretion is exponential, $M_{\rm BH} = M_{\rm BH,0}\exp(t/\tau)$, with a timescale $\tau \sim 4\times10^7\,(\epsilon/0.1)/\eta$ years, where $\epsilon = L/(\dot{M}_{\rm BH}c^2)$ is the radiation efficiency of

the accreting black hole and $\eta = L/L_{\rm Edd}$ is the ratio of the luminosity L to the Eddington luminosity. Therefore SMBHs with 10^7–10^9 solar masses need at least 10–20 e-foldings to assemble by accretion on seed black holes of $10{\sim}1000\,M_\odot$, which might be the compact remnants of an early generation of massive or very massive stars [23]. Provided enough gas were available in the surroundings to be swallowed by such a stellar mass black hole, and the efficiency of the black hole to absorb the gas flow were as high as assumed above, the time for its growth by accretion seems marginally short enough to explain the existence of quasars in the early Universe.

Fig. 1. A 3,700 light-year-diameter dust disk around the 300 million solar-mass black hole in the center of the elliptical galaxy NGC 7052 as observed by the Hubble Space Telescope. (Credits: Roeland P. van der Marel (STScI), Frank C. van den Bosch (University of Washington), and NASA)

A consistent and satisfactory picture of the formation process of quasar black holes has not been developed yet [39]. A variety of different routes were suggested (for a review, see Ref. [37]), including scenarios based on gas hydrodynamics, stellar dynamics, or combinations of both. Primordial gas clouds could collapse directly to SMBHs when their fragmentation is inhibited by radiation pressure or magnetic fields [31,22]. Alternatively, when angular momentum plays a role and the cooling timescale is much smaller than the viscous timescale, they might contract to form a supermassive disk [47,14]. If instead fragmentation of a primordial gas cloud occurred and a dense cluster of stars were born, stellar collisions and mergers might lead to a runaway growth of intermediate-mass black holes (e.g., Refs. [6,36,12,35]). A dense cluster composed of neutron stars or black holes as the compact remnants of massive stars might be driven by the secular "gravothermal catastrophe" to the point of a final relativistic instability that happens on a dynamical timescale [50,44] (see, however, Ref. [6] for arguments against this picture).

Some of the proposed scenarios are envisioned to lead to the build-up of a supermassive star (SMS) as an intermediate stage of the evolution before the

final gravitational instability sets in and the collapse to a SMBH takes place. Further growth of a seed black hole, possibly a SMBH, by accretion, could be linked to processes during the formation or evolution of the bulge of a galaxy (e.g., Refs. [42,46]). Galaxy formation or interaction could directly result in the black hole feeding that makes quasars shine, and bigger galaxies might be able to provide more fuel. This might explain why more massive galaxies contain more massive black holes [28].

2 Supermassive Stars: Some Basic Facts

Supermassive stars (SMSs) are equilibrium configurations that are dominated by radiation pressure. Their temperature is low enough that electron-positron pairs do not play a role. Baryons yield only a minor contribution to the equation of state. At some point of their evolution SMSs collapse due to a general relativistic gravitational instability [25,26,11,15,16,49,7,43].

SMSs can have masses between $\sim 10^4\,M_\odot$ and about $10^8\,M_\odot$. Since they are expected to be fully convective [43] (a formal argument can be found in Ref. [31]), they are isentropic and their structure can be well described by a Newtonian polytrope with $n = 3$ or $\gamma = 1 + 1/n = 4/3$. With their specific entropy being nearly constant, the adiabatic polytropic constant γ is roughly equal to the local adiabatic index $\Gamma = [\mathrm{d}(\ln P)/\mathrm{d}(\ln \rho)]_s$. To good accuracy the entropy per nucleon in a SMS, $s_{\rm SMS}$, is given by the radiation entropy (in units of Boltzmann's constant k)

$$\frac{s_{\rm SMS}}{k} \approx \frac{s_{\rm r}}{k} = (1.22 \times 10^{-22})\,\frac{T^3}{\rho} = 0.94\left(\frac{M}{M_\odot}\right)^{1/2}, \qquad (1)$$

where M is the mass of the star, ρ the density in $\mathrm{g\,cm^{-3}}$, and T the temperature in K (see, e.g., Refs. [43,21]). SMSs with large masses have entropies much higher than typical astrophysical plasmas. This suggests that dissipative processes (shocks, cloud-cloud collisions, turbulence) must be invoked for generating appropriate conditions for the formation of such supermassive equilibrium configurations.

The evolution of SMSs proceeds on a Kelvin-Helmholtz timescale and is driven by the loss of energy and entropy through radiation and — in case of rotation being important — the loss of angular momentum, e.g. via mass shedding. Because the pressure is dominated by radiation, the luminosity of SMSs is close to the Eddington limit,

$$L_{\rm SMS} = L_{\rm Edd} = \frac{4\pi G c M m_p}{\sigma_{\rm T}} = 1.3 \times 10^{38}\,\frac{M}{M_\odot}\,\mathrm{ergs\,s^{-1}}, \qquad (2)$$

with $\sigma_{\rm T}$ being the Thompson cross section and m_p the proton mass.

Although plasma corrections (due to nuclei and electrons[1]) and general relativistic effects are small, neither of both can be neglected for the evolution of a

[1] For reasons of simplicity, a pure hydrogen plasma is assumed here. The expressions for the general case can be found in Refs. [21,45]).

configuration which is so close to the pathological, i.e., dynamically marginally stable, case of a $\gamma = 4/3$ polytrope (for a discussion, see Ref. [43]). Pressure contributions by plasma components raise the adiabatic index of the equation of state, Γ, to a value above 4/3 [10]:

$$\Gamma_{\rm SMS} \,=\, 1 + \frac{P}{\varepsilon} \,\approx\, \frac{4}{3} + \frac{\beta}{6}\,. \tag{3}$$

Here ε is the total internal energy density without rest-mass energy, and the second expression is correct to first order in the ratio of the gas pressure to the radiation pressure, $\beta = P_{\rm g}/P_{\rm r} = 8/(s_{\rm r}/k) \ll 1$.

General relativity leads to the existence of a maximum for the equilibrium mass as a function of the central density for SMSs with constant entropy. This implies that general relativistic stars of mass M, which are supported both by radiation and gas pressure, have a maximum, i.e., "critical", central density:

$$\rho_{\rm crit} \,=\, 2\times 10^{18}\left(\frac{M}{M_\odot}\right)^{-7/2}\,{\rm g\,cm^{-3}}\,. \tag{4}$$

For higher central densities the nonlinear effects of gravity have a destabilizing influence to radial perturbations. The central temperature at the onset of the gravitational instability is

$$T_{\rm crit} \,=\, 2.5\times 10^{13}\left(\frac{M}{M_\odot}\right)^{-1}\,{\rm K}\,, \tag{5}$$

and the corresponding equilibrium energy can be found to be

$$E_{\rm crit} \,=\, -3.6\times 10^{54}\,{\rm ergs}\,, \tag{6}$$

which is independent of M. The redshift factor at the surface of a supermassive star (with radius $R = R_{\rm crit}$) at this point of the evolution is

$$\left(\frac{GM}{Rc^2}\right)_{\rm crit} \,=\, \frac{1}{2}\,\frac{R_{\rm s}}{R_{\rm crit}} \,=\, 0.63\left(\frac{M}{M_\odot}\right)^{-1/2}\,, \tag{7}$$

which is in the range 10^{-2}....10^{-4} for $M = 10^4\,M_\odot$....$10^6\,M_\odot$ and thus indeed very small so that the configuration is much larger than its Schwarzschild radius, $R_{\rm crit}/R_{\rm s} = 0.794\sqrt{M/M_\odot}$. Nevertheless, general relativity plays a crucial role for the evolution.

The gravitational instability sets in when the effective adiabatic index of the configuration (Eq. 3) drops below a critical value, which is approximately given by

$$\Gamma \,<\, \Gamma_{\rm crit} \,\approx\, \frac{2}{3}\,\frac{2-5\eta}{1-2\eta} \,+\, 1.12\,\frac{R_{\rm s}}{R}\,. \tag{8}$$

$R_{\rm s} = 2GM/c^2$ is the Schwarzschild radius of the star and $\eta = T/|W|$ is the ratio of the rotational energy to the gravitational potential energy. For $\eta = 0$, Eq. (8)

becomes $\Gamma_{\rm crit} = 4/3 + 1.12 R_{\rm s}/R$ (see Ref. [32] and references therein). Therefore the gravitational collapse begins when the plasma contribution to the equation of state does not raise the adiabatic index sufficiently above 4/3 to compensate for the destabilizing influence of general relativity. The latter grows as the radius of the star shrinks during its evolution. Rotation has a stabilizing effect and can hold up the collapse if

$$\eta \; > \; \eta_{\rm crit} \; \approx \; \frac{1}{2} \, \frac{4 - 3(\Gamma - 1.12 R_{\rm s}/R)}{5 - 3(\Gamma - 1.12 R_{\rm s}/R)} \, . \tag{9}$$

If $\eta > 0$ remains a constant during the equilibrium evolution, the final instability is again reached when the relativistic terms become too large.

Since the central density and temperature are higher for stars with smaller masses, and both increase during the quasistatic evolution, the creation of electron-positron pairs can be neglected for $M \gtrsim 10^4 \, M_\odot$ (i.e., $T \leq T_{\rm crit} \lesssim 2.5 \times 10^9 \, {\rm K}$; Eq. 5) [9]. A comparison of the nuclear energy generation rate with the photon luminosity (Eq. 2) shows that nuclear burning is also irrelevant prior to the gravitational instability for SMSs with masses in excess of a few $10^5 \, M_\odot$ [16,49].

While radiating energy at its Eddington limit, the SMS evolves on a timescale

$$t_{\rm KH} \; = \; \frac{|E_{\rm crit}|}{L_{\rm SMS}} \; = \; 2.8 \times 10^{16} \left(\frac{M}{M_\odot} \right)^{-1} {\rm s} \tag{10}$$

with essentially constant mass but decreasing entropy and energy until the critical configuration for the general relativistic instability is reached and the catastrophic collapse sets in. Only when the thermal (Kelvin-Helmholtz) timescale is longer than the hydrodynamical timescale,

$$t_{\rm hydro} \; \sim \; (G\rho)^{-1/2} \; = \; 2.7 \times 10^{-6} \left(\frac{M}{M_\odot} \right)^{7/4} {\rm s} \, , \tag{11}$$

there is an equilibrium phase of the evolution of the supermassive object. The two timescales become equal (about 10 years) for $M \sim 10^8 \, M_\odot$. Above this mass no hydrostatic phase is possible. More typical SMSs with $M \sim 10^6 \, M_\odot$ have a lifetime of about 1000 years.

Since SMSs are very close to the edge of instability, rotation can appreciably stretch their equilibrium evolution. Considering the secular evolution of a uniformly rotating configuration along the mass-shedding sequence, Baumgarte and Shapiro [5] found a lifetime independent of the stellar mass, $t \approx 9 \times 10^{11} \, s$. Moreover, they showed that the key nondimensional ratios $R/R_{\rm s}$, $T/|W|$, and $Jc/(GM^2)$ (J is the angular momentum) for a maximally and rigidly rotating $n = 3$ polytrope at the onset of radial instability are universal numbers, independent of the mass, spin, radius, or history of the star:

$$\left(\frac{T}{|W|} \right)_{\rm crit} \approx \, 0.009 \, , \quad \left(\frac{Jc}{GM^2} \right)_{\rm crit} \approx \, 0.97 \, , \quad \left(\frac{R_{\rm p}}{R_{\rm s}} \right)_{\rm crit} \approx \, 214 \, , \tag{12}$$

with the polar radius $R_{\rm p}$ being roughly 2/3 of the equatorial radius $R_{\rm e}$. This deformation reduces the luminosity by about 36% below the usual Eddington

luminosity of a corresponding nonrotating star [4]. The effects of differential rotation, where mass loss during the quasi-stationary evolution could be ignored, were discussed by New and Shapiro [33].

3 The Death of Supermassive Stars

Driven by energy loss through radiation and angular momentum loss due to mass shedding, SMSs contract slowly in a quasi-static manner and approach the point of dynamical instability as a consequence of the increasing effects of general relativity. The subsequent catastrophic collapse can lead to the formation of a SMBH [1] or, for sufficiently large initial metallicity, to a violent explosion that is powered by the release of nuclear energy through hydrogen burning in the CNO cycle [8,2,17,18,21].

These events are associated with the emission of gigantic amounts of energy in neutrinos [48], a fact that has nourished speculations that SMSs collapsing to black holes might be the sources of cosmic gamma-ray bursts [20]. In the case of rotationally deformed configurations, which might encounter a dynamical bar mode instability that triggers the growth of nonaxisymmetric bars, the generation of long-wavelength gravitational waves can be expected. Such gravitational waves could be detectable by future space-based laser interferometers like LISA [5,33,40]. Moreover, SMSs that were disrupted by explosions might have contributed to the enrichment of the gas in the young Universe with elements heavier than helium, in particular of comparatively rare isotopes like ^{13}C, ^{15}N, ^{17}O, and ^{22}Ne [3], and in case of SMSs with high metallicities of ^{26}Al [24].

The last investigation of nuclear burning during the collapse and explosion of SMSs was undertaken by Fuller et al. [21]. They performed hydrodynamical calculations with a post-Newtonian approximation to general relativistic gravity, used a detailed equation of state including electron-position pairs, and took into account photon and neutrino losses as well as all nuclear reactions for describing hydrogen burning by the CNO cycle (limited by β^+ decays of ^{14}O and ^{15}O) and by the rapid proton capture (rp-) process that characterizes hydrogen burning at very high temperatures ($T \gtrsim 10^9\,\mathrm{K}$; at such temperatures, however, neutrino losses become dominant). Considering nonrotating configurations, Fuller et al. [21] found that stars with a mass $M \gtrsim 10^5\,M_\odot$ and initial metallicities $Z \lesssim 0.005$ do not explode, whereas objects with $Z \gtrsim 0.005$ (a value near the solar mass fraction of heavy elements!) do explode. The explosion energies range from $2 \times 10^{56}\,\mathrm{ergs}$ for stars of mass $M \approx 10^5\,M_\odot$ to $2.5 \times 10^{57}\,\mathrm{ergs}$ for $M \approx 10^6\,M_\odot$, and the photon luminosities can exceed $10^{45}\,\mathrm{ergs\,s^{-1}}$ for a period of more than ten years. The nucleosynthesis in exploding SMSs is characterized by the production of a large amount of ^{4}He and trace amounts of ^{15}N and ^{7}Li. Deuterium production turned out to be negligible because this nucleus is too fragile to survive the high temperatures during the explosion of supermassive objects (see, however, Ref. [19] for neutrino-induced deuterium generation in the ejected envelope of exploding SMSs). Since zero metallicity (nonrotating) SMSs do not blow up, they, however, cannot be considered as a source of pre-galactic helium.

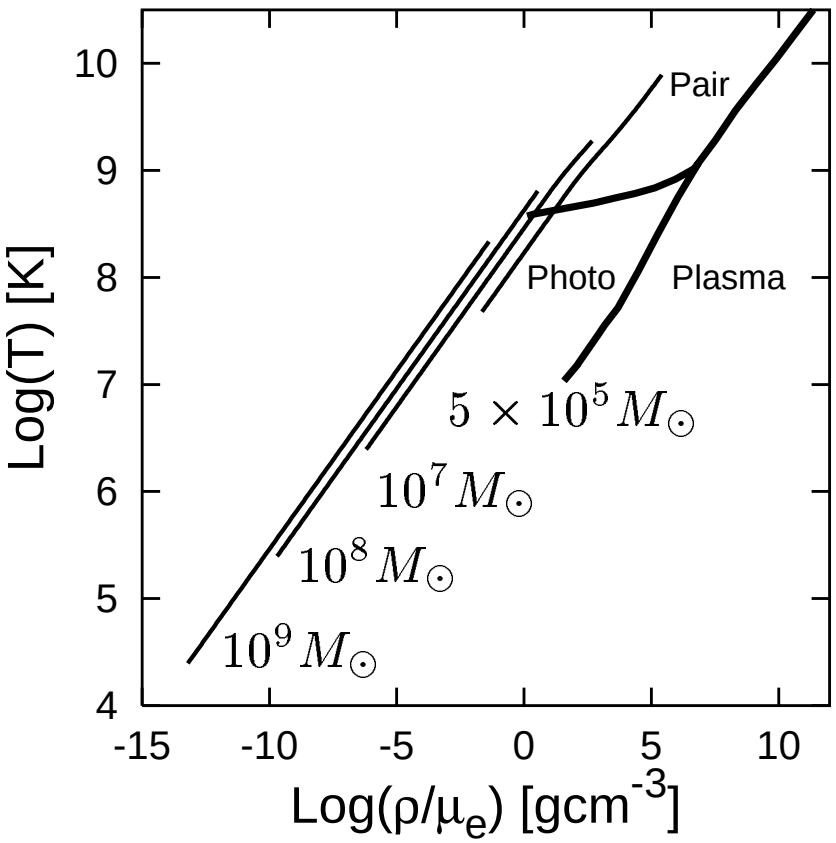

Fig. 2. Evolutionary tracks of the center of collapsing SMSs with different masses in the ρ-T-plane (μ_e is the mean molecular weight). Initially the photo-neutrino production yields the major contribution to the neutrino loss, during the later phases of the collapse it is the pair annihilation process. Plasmon neutrinos are negligible

Recently Linke et al. [29,30] have performed simulations in full general relativity of the collapse of nonrotating SMSs to black holes with the aim to calculate in detail the neutrino (and antineutrino) emission of such events until the point when the emission is quickly terminated by the formation of the event horizon. Their models also included electron-positron pairs and plasma contributions besides photons in the equation of state and were focused on cases where the energy release by nuclear burning is unimportant because it is dwarfed by neutrino losses. In Fig. 2 the evolutionary tracks of the central density and temperature of SMSs in the mass range between $5 \times 10^5\, M_\odot$ and $10^9\, M_\odot$ are plotted on top of the regions of dominant energy loss by the neutrino-antineutrino pair production

through the photo-neutrino process ($\gamma + e^{\pm} \rightarrow e^{\pm} + \nu + \bar{\nu}$), electron-positron pair annihilation ($e^- + e^+ \rightarrow \nu + \bar{\nu}$), and plasmon decay ($\widetilde{\gamma} \rightarrow \nu + \bar{\nu}$).

Energy losses by neutrino production become important only during the later stages of the collapse. Initially the photo-neutrino process plays the dominant role, whereas shortly before the black hole forms, when most of the neutrino emission occurs, the temperature is so high that the pair-neutrino process takes over. Plasmon neutrinos yield a negligible contribution in all cases. The neutrino emission rates are extremely temperature dependent. The energy production rate by electron-positron annihilation, Q_ν, rises like T^9 above the threshold temperature for pair formation and even more steeply ($Q_\nu \propto T^{20}$) for temperatures just below 10^9 K when e^+e^- pair creation sets in [27].

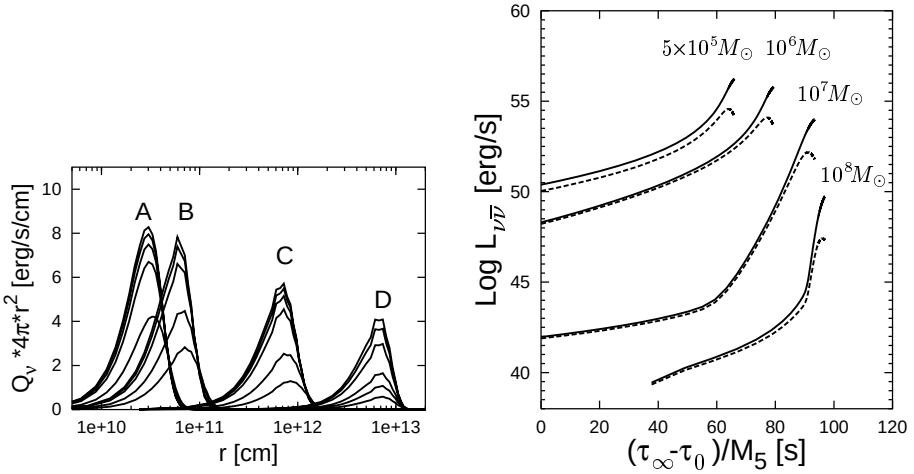

Fig. 3. Radial profiles of the neutrino plus antineutrino emission rate (times $4\pi r^2$; left) and luminosities of neutrinos plus antineutrinos as a function of time (right) for collapsing SMSs with different masses. The left plot gives the quantity $\mathrm{d}L_{\nu\bar{\nu}}(r)/\mathrm{d}r$ for $M = 5\times10^5\,M_\odot$ (A), $10^6\,M_\odot$ (B), $10^7\,M_\odot$ (C), and $10^8\,M_\odot$ (D) for different epochs of the model evolution with the end of the simulations being represented by the uppermost lines. The corresponding scaling factors are 5×10^{44} (A), 10^{44} (B), $2\times10^{41}\,M_\odot$ (C), and 2×10^{36} (D), respectively. In the right figure the dashed lines include Doppler shifts and general relativistic redshift effects, the solid lines do not. The time is measured in seconds with τ_∞ being the proper time for an observer at infinity, shifted by the overall collapse timescale ($\tau_0 = 8\times10^5$ s, 1.7×10^6 s, 8.0×10^7 s, and 3.2×10^9 s, respectively) and scaled by $M_5 = M/(10^5\,M_\odot)$

Although enormous amounts of energy are radiated away in neutrinos, these energy losses are small compared to the internal energy or the gravitational potential energy of the star. The neutrino losses are therefore essentially irrelevant in the energy budget and the collapse can well be considered as adiabatic. It proceeds nearly homologously so that the density profile evolves in a self-similar

manner. Deviations from this ideal behaviour of a Newtonian $n = 3$ polytrope at a later stage of the collapse are caused by the increasing influence of general relativity and to a minor degree also by the possible formation of electron-positron pairs and the corresponding reduction of the adiabatic index. Except for such effects that are associated with the equation of state or with the neutrino emission — both of which are very sensitive to the maximum value of the temperature that is reached during the implosion — the collapse of SMSs of different masses is found to be very similar. The stellar mass therefore simply acts as a scaling parameter, a fact which will be made use of in the following discussion.

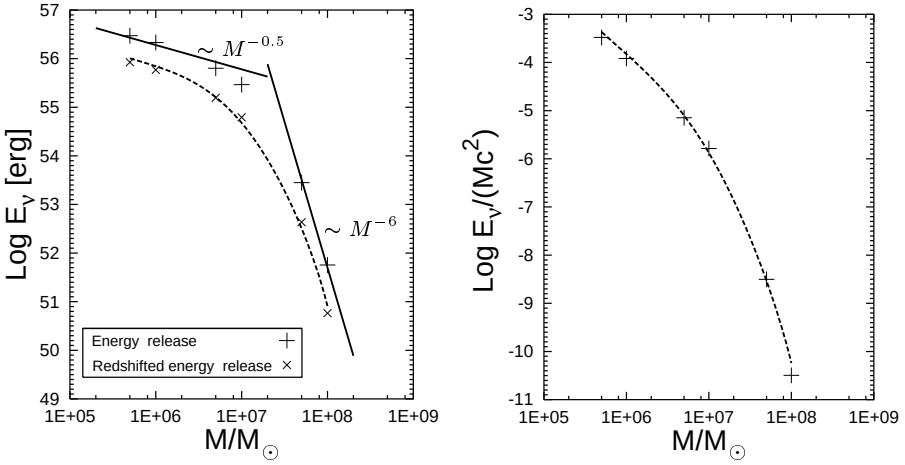

Fig. 4. Total energy release in form of neutrinos during the collapse of SMSs to SMBHs (left). The mass of the star is given on the abscissa. The dashed curve interpolates the computed values (symbols) which include the effects of Doppler shift and general relativistic redshift, while the solid lines interpolate the results for the integral energies as measured by local observers. The right plot shows the efficiency of the conversion of rest-mass energy to neutrinos, $E_\nu/(Mc^2)$. In case of less massive stars the higher core temperatures before black hole formation imply much larger values for the total energy emitted in neutrinos and for the conversion efficiency

The collapse timescale $t_{\rm coll}$ is roughly proportional to $R_{\rm s}/c \propto M$ and lasts between about 9 days for a SMS with $5 \times 10^5\,M_\odot$ and several years for $10^7\,M_\odot$ stars. For more massive stars a meaningful calculation of the duration of the phases of contraction and implosion requires the inclusion of photon emission (cf. Eq. 10), which in fact was ignored in our models. The collapse of the innermost $\sim 25\%$ of the mass proceeds in a nearly coherent way with an approximately homologous velocity profile. This part of the star therefore forms a black hole first and determines the radius of the innermost apparent horizon, which is proportional to M.

Because the highest temperatures are reached at the end of the collapse, the time interval of strongest neutrino emission is also given by $t_{\rm em} \sim R_{\rm s}/c \propto M$. The peak of the neutrino production is located in a shell just outside the innermost apparent horizon (Fig. 3). The corresponding "neutrino emission radius" is therefore also proportional to the event horizon of the SMS, $R_\nu \propto R_{\rm s} \propto M$ (Fig. 3) and thus much smaller than the stellar radius (Eq. 7). Since the collapse proceeds very nearly adiabatically ($T^3/\rho \approx$ const; Eq. 1), one can also easily estimate how the maximum core temperature, which determines the neutrino emission, depends on the mass of the star. Mass conservation implies for the final density $\rho_{\rm f} \sim (R_{\rm crit}/R_{\rm s})^3 \rho_{\rm crit}$ with $R_{\rm crit}/R_{\rm s} \propto M^{1/2}$ (Eq. 7) and $\rho_{\rm crit} \propto M^{-7/2}$ (Eq. 4). Using this in Eq. (1) one finds for the final temperature $T_{\rm f} \propto M^{-1/2}$ [45]. Neutrinos are emitted with a mean energy $\langle \epsilon_\nu \rangle$ that scales with the stellar temperature in the main production region. A detailed discussion yields $\langle \epsilon_\nu \rangle \sim 6kT_{\rm f}$ [45].

The maximum neutrino plus antineutrino luminosity decreases steeply with higher stellar masses:

$$L_{\nu\bar{\nu}} \sim Q_\nu \frac{4\pi}{3} R_\nu^3 \propto \begin{cases} M^{-3/2} & \text{for } 10^5\,M_\odot \lesssim M \lesssim 5\times10^6\,M_\odot\,, \\ M^{-7} & \text{for } 5\times10^7\,M_\odot \lesssim M \lesssim 10^8\,M_\odot\,. \end{cases} \tag{13}$$

The right plot in Fig. 3 shows this trend. The change in the slope of the luminosities as a function of time that is visible for the cases $M = 10^7\,M_\odot$ and $M = 10^8\,M_\odot$ near $L_{\nu\bar{\nu}} \sim 10^{43}\,{\rm ergs\,s^{-1}}$ is associated with the transition from the photo-neutrino dominated to the pair-neutrino dominated regime (compare Fig. 2). The total energy release in neutrinos and antineutrinos exceeds 10^{56} ergs for SMS with $M \lesssim 10^6\,M_\odot$. Stars with smaller masses are the clearly stronger neutrino sources:

$$E_\nu \sim L_{\nu\bar{\nu}}\,t_{\rm em} \propto \begin{cases} M^{-1/2} & \text{for } 10^5\,M_\odot \lesssim M \lesssim 5\times10^6\,M_\odot\,, \\ M^{-6} & \text{for } 5\times10^7\,M_\odot \lesssim M \lesssim 10^8\,M_\odot\,. \end{cases} \tag{14}$$

As displayed in Fig. 4, the observable energies are somewhat lowered by effects due to Doppler shift and gravitational redshift. SMSs near the lower end of the investigated mass range convert a fraction of more than 10^{-4} of their rest-mass energy to neutrinos, whereas it is less than 10^{-10} in case of stars with $M = 10^8\,M_\odot$ (right plot in Fig. 4).

4 Conclusions

Although the energy emitted in neutrinos is huge in case of SMSs that form SMBHs with masses $M \lesssim 10^7\,M_\odot$, it is very unlikely that these neutrinos can produce a highly relativistic outflow to power cosmic gamma-ray bursts. On the one hand, the efficiency of neutrino-antineutrino annihilation to electron-positron pairs is extremely low ($\lesssim 10^{-5}$ of the neutrino energy are converted to $e^\pm$ pairs [29,30]). On the other hand, 99.8% of this energy are deposited in the close vicinity of the neutrino emitting shell, i.e. in matter which is swept inward in the collapse with velocities up to 60% of the speed of light. The

deposited energy is much too small to invert this rapid infall and to create a hightly relativistic outflow. A black hole-disk configuration might provide a more suitable environment, but is very unlikely to form even in the case of the collapse of SMSs with rotation [40]. Moreover, SMSs as gamma-ray burst sources are unable to account for the short-time variability of the observed emission, which is directly linked to the activity of the source [41]. This requires a very compact energy source with a size which is typical of a neutron star or stellar mass black hole.

Investigations of the evolution and collapse of nonrotating SMSs are a somewhat academic exercise. Since the configurations are so close to dynamical instability, a small amount of rotation may have a significant impact. This has indeed been found for the quasi-static evolution of uniformly rotating [5] and differentially rotating stars [33]. The collapse of stars which rotate uniformly at the onset of gravitational instability, however, turns out to be very similar to the nonrotating case. Saijo et al. [40] found that such a collapse is likely to form a SMBH coherently, with almost all of the matter falling into the hole on a dynamical timescale and only very little matter possibly ending up in a disk. They did not discover an unstable growth of a nonaxisymmetric bar. Certainly such investigations of the death of SMSs should be extended to differentially rotating configurations and to models which include a detailed microphysical description of the equation of state (instead of using a simple Γ-law equation $P = (\Gamma - 1)\varepsilon$). Moreover, the neutrino emission and possible energy release by nuclear burning should be taken into account. The latter might be more important for rotating SMSs than for nonrotating ones. Centrifugal forces might hold up the collapse long enough for nuclear reactions to generate sufficient energy to influence the dynamics even in case of zero initial metallicity [21].

Acknowledgements. Stimulating conversations with T. Abel and A. Heger are acknowledged. The author thanks F. Linke, J.A. Font, E. Müller and P. Papadopoulos for a pleasant collaboration and is very grateful to R. Sunyaev for inspiring discussions and the opportunity to present this review at the conference "Lighthouses of the Universe". This work was supported by the Sonderforschungsbereich 375 "Astroparticle Physics" of the Deutsche Forschungsgemeinschaft.

References

1. I. Appenzeller, K. Fricke: Astron. Astrophys. **18**, 10 (1972)
2. I. Appenzeller, K. Fricke: Astron. Astrophys. **21**, 285 (1972)
3. J. Audouze, K.J. Fricke: Astrophys. J. **186**, 239 (1973)
4. T.W. Baumgarte, S.L. Shapiro: Astrophys. J. **526**, 937 (1999)
5. T.W. Baumgarte, S.L. Shapiro: Astrophys. J. **526**, 941 (1999)
6. M.C. Begelman, M.J. Rees: Mon. Not. R. Astr. Soc. **185**, 847 (1978)
7. G.S. Bisnovatyi-Kogan, Ya.B. Zel'dovich, I.D. Novikov: Soviet Astronomy–AJ **11**, 419 (1967)
8. G.S. Bisnovatyi-Kogan: Soviet Astronomy–AJ **12**, 58 (1968)

9. J.R. Bond, A.D. Arnett, B.J. Carr: Astrophys. J. **280**, 825 (1984)
10. S. Chandrasekhar: *An Introduction to the Study of Stellar Structure* (University of Chicago Press, Chicago 1939)
11. S. Chandrasekhar: Astrophys. J. **140**, 417 (1964)
12. T. Ebisuzaki, J. Makino, T.G. Tsuru et al: Astrophys. J. **562**, L19 (2001)
13. A. Eckart, R. Genzel: Mon. Not. R. Astr. Soc. **284**, 576 (1997) R. Genzel, A. Eckart, T. Ott, F. Eisenhauer: Mon. Not. R. Astr. Soc. **291**, 219 (1997)
14. D.J. Eisenstein, A. Loeb: Astrophys. J. **443**, 11 (1995)
15. W.A. Fowler: Rev. Mod. Phys. **36**, 545, 1104err (1964)
16. W.A. Fowler: Astrophys. J. **144**, 180 (1966)
17. K.J. Fricke: Astrophys. J. **183**, 941 (1973)
18. K.J. Fricke: Astrophys. J. **189**, 535 (1974)
19. G.M. Fuller, X. Shi: Astrophys. J. **487**, L25 (1997)
20. G.M. Fuller, X. Shi: Astrophys. J. **502**, L5 (1998)
21. G.M. Fuller, S.E. Woosley, T.A. Weaver: Astrophys. J. **307**, 675 (1986)
22. O.Y. Gnedin: Class. Quantum Grav. **18**, 3983 (2001)
23. A. Heger, S.E. Woosley: Astrophys. J., in press (2002) (`astro-ph/0107037`)
24. W. Hillebrandt, F.-K. Thielemann, N. Langer: Astrophys. J. **321**, 761 (1987)
25. F. Hoyle, W.A. Fowler: Mon. Not. R. Astr. Soc. **125**, 169 (1963)
26. I. Iben: Astrophys. J. **138**, 1090 (1963)
27. N. Itoh, H. Hayashi, A. Nishikawa, Y. Kohyama: Astrophys. J. Suppl. **102**, 411 (1996)
28. J. Kormendy, D. Richstone: Ann. Rev. Astron. Astrophys. **33**, 581 (1995) J. Kormendy, K. Gebhardt: 'Supermassive Black Holes in Galactic Nuclei'. In: *Proceedings of The 20th Texas Symposium on Relativistic Astrophysics, Austin, Texas, Dec. 10–15, 2000*, ed. by H. Martel, J.C. Wheeler, in press (2002) (`astro-ph/0105230`)
29. F. Linke: General Relativistic Simulation of Collapsing Supermassive Stars. Diploma Thesis, Technical University, Munich (2000)
30. F. Linke, J.A. Font, H.-T. Janka, E. Müller, P. Papadopoulos: Astron. Astrophys. **376**, 568 (2001)
31. A. Loeb, F.A. Rasio: Astrophys. J. **432**, 52 (1994)
32. C.W. Misner, K.S. Thorne, J.A. Wheeler: *Gravitation* (W.H. Freeman and Company, San Francisco 1973)
33. K.C.B. New, S.L. Shapiro: Astrophys. J. **548**, 439 (2001)
34. M.J. Page, J.A. Stevens, J.P.D. Mittaz, F.J. Carrera: Science **294**, 2516 (2001)
35. S.F. Portegies Zwart, S.L.W. McMillan: Astrophys. J., submitted (`astro-ph/-0201055`)
36. G.D. Quinlan, S.L. Shapiro: Astrophys. J. **356**, 483 (1990)
37. M.J. Rees: Ann. Rev. Astron. Astrophys. **22**, 471 (1984)
38. M.J. Rees: 'Astrophysical Evidence for Black Holes'. In: *Black Holes and Relativistic Stars, Proceedings of Chandrasekhar Memorial Conference, Chicago, Dec. 1996*, ed. by R.M. Wald (University of Chicago Press, Chicago 1998) pp. 79–100
39. M.J. Rees: 'Supermassive Black Holes: Their Formation, and Their Prospects as Probes of Relativistic Gravity'. In: *Black Holes in Binaries and Galactic Nuclei, Proceedings of ESO Workshop, Garching, Germany, Sept. 6–8, 1999*, ed. by L. Kaper, E.P.J. van den Heuvel, P.A. Woudt (Springer, New York 2001) pp. 351–364
40. M. Saijo, T.W. Baumgarte, S.L. Shapiro, M. Shibata: Astrophys. J., in press (2002)
41. R. Sari, T. Piran: Astrophys. J. **485**, 270 (1997)

42. H. Schulz, S. Komossa: 'Formation of Massive Black Holes in Early Mergers?'. In: *Trends in Astrophysics and Cosmology, Proceedings of Workshop, Bad Honnef, Germany, Aug. 24–28, 1998*, ed. by W. Kundt, C.v.d.Bruck (Lecture Notes in Physics, Springer, Heidelberg) in press (`astro-ph/9905118`)
43. S.L. Shapiro, S.A. Teukolsky: *Black Holes, White Dwarfs, and Neutron Stars* (John Wiley & Sons, New York 1983)
44. S.L. Shapiro, S.A. Teukolsky: Astrophys. J. **292**, L41 (1985)
45. X. Shi, G.M. Fuller: Astrophys. J. **503**, 307 (1998)
46. M. Umemura: Astrophys. J. **560**, L29 (2001)
47. R.V. Wagoner: Ann. Rev. Astron. Astrophys. **7**, 553 (1969)
48. S.E. Woosley, J.R. Wilson, R. Mayle: Astrophys. J. **302**, 19 (1986)
49. Ya.B. Zel'dovich, I.D. Novikov: *Stars and Relativity* (University of Chicago Press, Chicago 1971)
50. Ya.B. Zel'dovich, M.A. Podurets: Soviet Astronomy **9**, 742 (1965)

This figure "jankahf1.png" is available in "png" format from:

http://arXiv.org/ps/astro-ph/0202028v1